Activation of Osteoblastic Function on Titanium Surface with Titanium-Doped Hydroxyapatite Nanoparticle Coating: An In Vitro Study

Masahiro Nakazawa, DDS, PhD[1]/Masahiro Yamada, DDS, PhD[2]/Masato Wakamura, PhD[3]/
Hiroshi Egusa, DDS, PhD[4]/Kaoru Sakurai, DDS, PhD[5]

Purpose: *Titanium-doped hydroxyapatite (TiHA) nanoparticles contain titanium atoms in the hydroxyapatite lattice, which can physicochemically functionalize the titanium surface without modification of the surface topography. This study aimed to evaluate the physicochemical properties of machined or microroughened titanium surfaces coated with TiHA nanoparticles and the functions of osteoblasts cultured on them.* ***Materials and Methods:*** *Titanium disks with commercially available surface topography, such as machined or sandblasted, large-grit, and acid-etched (SLA) surfaces, were coated with TiHA. The disks with original or TiHA-coated surfaces were evaluated in topography, wettability, and chemical composition. Osteoblastic cells from rat femurs were cultured on the disks and evaluated in proliferation and differentiation.* ***Results:*** *TiHA coating changed from hydrophobicity to hydrophilicity on both machined and SLA surfaces. Calcium and phosphate atoms were detected all over the surface with TiHA coating regardless of the surface topography. However, the considerable change in the inherent surface topographies was not observed on both types of surfaces after TiHA coating. Osteoblastic proliferative activity at day 4 was increased by TiHA coating on both types of surfaces. TiHA coating did not enhance expressions of bone matrix–related genes such as osteocalcin, osteopontin, bone sialoprotein, alkaline phosphatase, and collagen I. However, depositions of collagen, osteocalcin, and calcium in the culture at days 7 and 20 were increased on both types of surface topographies with TiHA coating.* ***Conclusion:*** *TiHA coating enhanced extracellular matrix formation on smooth and microroughened titanium surfaces by increasing osteoblastic proliferative activity without the deterioration of differentiation through hydrophilic and chemical functionalization.* Int J Oral Maxillofac Implants 2017;32:779–791. doi:10.11607/jomi.5421

Keywords: *calcium, osseointegration, osteoblastic culture, surface topography, wettability*

Surface properties regulate osteoblastic cellular behavior and function on the surface of an implant, thereby determining its osseointegration capability.[1]

[1]Postdoctoral Student, Department of Removable Prosthodontics and Gerodontology, Tokyo Dental College, Tokyo, Japan.
[2]Senior Assistant Professor, Division of Molecular and Regenerative Prosthodontics, Tohoku University Graduate School of Dentistry, Sendai, Japan.
[3]Research Manager, Device Innovation Project, Device & Materials Laboratory, Fujitsu Laboratories Ltd, Kanagawa, Japan.
[4]Professor, Division of Molecular and Regenerative Prosthodontics, Tohoku University Graduate School of Dentistry, Miyagi, Japan.
[5]Professor, Department of Removable Prosthodontics and Gerodontology, Tokyo Dental College, Tokyo, Japan.

Correspondence to: Dr Masahiro Yamada, Senior Assistant Professor, Division of Molecular and Regenerative Prosthodontics, Tohoku University Graduate School of Dentistry, 4-1, Seiryouchou, Aoba-ku, Sendai, Japan, 980-8575. Fax: (+81) 022-717-8367. Email: masahiro.yamada.a2@tohoku.ac.jp

Surface properties of biomaterials are currently categorized into surface topography and physicochemical properties such as wettability, chemical properties, and electric charge.[2,3] Many studies have provided evidence of surface topography substantially modulating osteoblastic cellular behavior and determining the osseointegration capability of an implant.[2] It has been established that a micro roughened to submicroroughened titanium surface enhances and accelerates extracellular matrix formation and mineralization by osteoblastic cells compared with a machined surface where cellular proliferation predominates rather than differentiation.[4] Consequently, a microroughened to submicroroughened titanium surface enhances osseointegration strength with an increase of bone-to-implant contact and formation of harder and stiffer bone tissue.[5]

In contrast, the effectiveness of currently available physicochemical surface modification for osseointegration remains uncertain. For example, it is generally known that a hydrophilic surface has an advantage

over a hydrophobic surface during deposition of extracellular matrix onto the material surface.[6] This is based on the prevention of microbubble formation[3] and the hiding of the adhesion motif of extracellular matrix by the collapse of the three-dimensional (3D) structure[7] on the hydrophobic surface. However, the adhesive strength between the deposited protein and hydrophilic surface is generally weak, and this principle is applied on a temperature-responsive culture plate in the field of tissue engineering.[8] In contrast, a chemical property of titanium surface enables modulation of the cellular attachment by a biochemical or bioelectrical mechanism. Cell-adhesive molecules have a selective affinity for certain functional groups on the surface, such as hydroxyl, amino, and carboxyl groups,[9,10] but not the methyl group.[11] In addition, the polarity of the extracellular matrix allows electrostatic attraction and direct binding to a positively charged surface[12] or indirect binding to a negatively charged surface via a divalent cation bridge.[13] However, these physicochemical surface properties may require synergistic interaction for the enhancement of osseointegration capability of the titanium surface beyond surface topography. In fact, superhydrophilicity did not increase osteoblastic cellular attachment and adhesion on the microroughened titanium surface without reduction of the surface carbon atom indicating methyl group.[14] Sandblasting with a large-grit and acid-etched implant modified with hydrophilication did not result in a difference in the final bone-to-implant contact ratio compared with the original surface.[15]

The next generation of hydroxyapatite material is titanium-doped hydroxyapatite [TiHA; $Ca_9Ti_1(PO_4)_6(OH)_2$]. The material is constructed by incorporation of the titanium ion (Ti^{4+}) into hydroxyapatite [$Ca_{10}(PO_4)_6(OH)_2$] (HA) based on the tolerance of the Ca site in the HA structure to ionic substitution with various divalent and trivalent cations.[16–21] TiHA is known to be inherently excited sufficiently in response to the bacterial effect under dark conditions, in contrast to the TiO_2 particle.[22] TiHA exhibits a hydrophilic status (about 40 degrees in water contact angle) regardless of ultraviolet irradiation.[23] This indicated that TiHA becomes inherently excited to produce free radicals and enables the maintenance of hydrophilicity. In addition, TiHA possessed inherent bipolarity as HA material with the Ca^{2+} and PO_4^{3-} ion (C and P) sites. Moreover, TiHA can be synthesized as various forms from plates to nanoparticles. Therefore, it was hypothesized that TiHA provides physicochemical properties to a titanium surface without topographic change and achieves substantial synergistic enhancement of osseointegration capability of the surface topography when the material is applied as titanium surface coating. This in vitro study aimed to evaluate the effect of TiHA coating onto a machined or microroughened titanium surface on osteoblastic cellular proliferation, and differentiation on the surface in association with the consideration of topographic and physicochemical changes on the surface.

MATERIALS AND METHODS

TiHA Particles

TiHA particles were obtained from Fujitsu Laboratories Ltd. The methodology to construct TiHA particles was based on hydrothermal synthesis and was reported previously.[24] Briefly, $Ca(NO_3)_2$ and $Ti(SO_4)_2$ were dissolved in deionized distilled water (ddH_2O), free from CO_2. The atomic ratio of Ti/(Ca + Ti) and pH in the solution was 0.1 and 9.0, respectively. The TiHA particles were generated by storing the suspension in a Teflon chamber at 100°C for 6 hours. The particles were filtered off, washed with ddH_2O, and finally dried at 70°C for 24 hours in the atmosphere. The TiHA particles were sintered at 650°C for 1 hour. The appearance was a white color. Transmission electron microscopic analysis (JEM-2100, JEOL Ltd) demonstrated that the TiHA exhibited an elliptical form with approximately 50 to 100 nm in major axis (Figs 1a and 1b). The crystal architecture was characterized by replacement of the titanium ion with the columnar or screw-axis calcium ion within a hexagonal lattice structure. The conceptual scheme of the TiHA-crystal architecture is shown in Fig 1c.

Titanium Disk Sample

Grade 4 titanium disks (the standards as ASTM F67 and ISO 5832_2) with machined or microroughened (sandblasted with large grits and thermally acid etched [SLA]) titanium disks with a 15.0 mm diameter were supplied by Thommen Medical AG. The microroughened surface was fabricated by sandblasting with large grits of aluminum oxide particles followed by etching in a mixture of hydrochloric and sulfuric acid at elevated temperature. TiHA coating was performed on both surface types at Fuji Kagaku Corp. Briefly, the disks were spin coated with TiHA sol/gel solution sequentially at 1,000 rpm for 40 seconds and 2,000 rpm for 5 seconds so as to be 150 to 200 nm in final thickness, using a spin coater (Opticoat MS-A150, MIKASA Co. Ltd). The coating thickness was checked with a laser microscope (LEXT OLS4000, Olympus). The condition of the coating in this study was determined by evaluation of the number of osteoblastic cells on the machined surface as hereafter described. Coating conditions tested were followed: *(1)* single spin coating with a low concentration of TiHA-coating solution in ethanol and 2-ethoxyethanol (3.85% w/w of TiHA in final concentration); *(2)* single spin coating with a high concentration

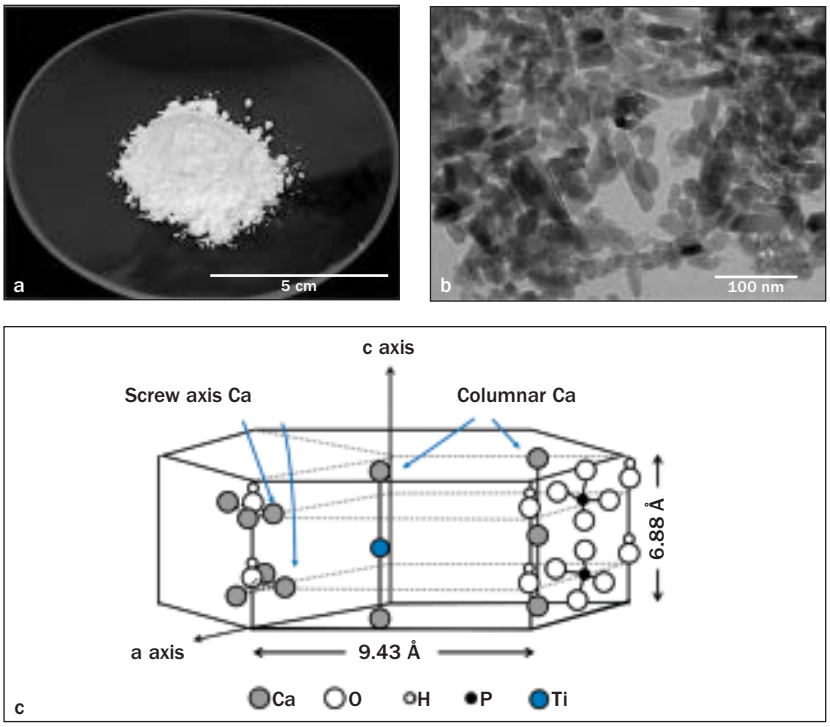

Fig 1 *(a)* Macroscopic and *(b)* TEM images of TiHA particles used in this study. *(c)* Schema of crystal structure of TiHA based on data of powder neutron diffraction obtained from Fujitsu Laboratories Ltd. Note that the doped titanium ion tended to replace an arbitrary columnar calcium ion. The speculated chemical formula was $Ca_9Ti_1(PO_4)_6(OH)_2$.

of TiHA-coating solution (19.25% w/w of TiHA in final concentration); *(3)* double spin coating with a low concentration of TiHA-coating solution (3.85% w/w of TiHA in final concentration). After coating, the disks were sintered at 500°C for 15 minutes. The disks were stored in the dark, before use. Single spin coating with a low concentration of TiHA solution was employed based on the results in the present study.

Surface Characterization

The topographic features at the micron level on each titanium surface were evaluated using a 3D-measuring laser microscope with a cutoff value of 8 μm and a measurement length of 120 μm. In addition, topographic changes at the nanolevel after TiHA coating were evaluated on the machined surface using a scanning probe microscope (SPM) (Nanocute, Seiko Instruments Inc) with a measurement length of 2 μm. Scanning electron microscopy (SEM; XL30, Philips) and an electron probe microanalyzer (EPMA; JXA-8200, JEOL Ltd) conducted topographic and elemental analyses. The wettability of each surface was measured as the contact angle of a 10-μL deionized distilled water droplet placed on the surface. Measurements were taken at 5 seconds after application of the droplet. Subsequently, the contact angle was calculated using ImageJ (National Institutes of Health). For the surface roughness measurements, three areas were measured per sample, and the data were averaged. Three independent samples were utilized for all repeated measurements.

Rat Osteoblastic Cell Culture

Rat bone marrow stromal cells were isolated from the femurs of 8-week-old male Sprague-Dawley rats. The cells were grown and underwent induction of osteoblastic differentiation in alpha-modified Eagle's medium (α-MEM) supplemented with 10% fetal bovine serum, 50 mg/mL ascorbic acid, 10 mM Na-beta-glycerophosphate, 10^{-8} M dexamethasone, and antibiotic-antimycotics in a humidified atmosphere of 95% air and 5% CO_2 at 37°C until 80% confluency. The passage was performed two times. Then, the cells were detached using 0.25% trypsin 1 mM tetrasodium ethylenediaminetetraacetic acid (EDTA) and seeded onto the titanium disks that had either a machined surface or microroughened surface, with or without TiHA coating, at a density of 3×10^4 cells/cm^2 in a 24-well culture plate. The culture medium was renewed every 3 days. The protocol was approved by the Animal Research Committee of Tokyo Dental College (Protocol No. 262604).

Evaluation of Cell Number and Proliferation

The number of cells on the surfaces was evaluated by WST-1 assay (Roche Applied Science). Each culture was incubated at 37°C for 4 hours in 0.5 mL fresh

culture media containing 50 μL of WST-1 reagent. Color change of the media was measured by colorimetry at 420 nm using a microplate reader (SpectraMax M5, Molecular Devices, LLC). The cell proliferation was measured by bromodeoxyuridine (BrdU). At day 4, a 100 mM BrdU solution (50 μL) (Roche Diagnostics) was added to the culture wells and incubated for 10 hours. After denaturing DNA, the cultures were incubated with anti-BrdU antibody conjugated with peroxidase for 90 minutes and exposed to tetramethylbenzidine (TMB) for color development. Absorbance was measured using a microplate reader at 370 nm.

Gene Expression Analysis

Gene expression was analyzed on days 10 and 20 using reverse-transcriptase polymerase chain reaction (PCR). The total RNA in these cultures was extracted using TRIzol (Invitrogen) and a purification column (RNeasy, Qiagen). Following DNAse I treatment, reverse transcription of 0.5 mg total RNA was performed using MMLV reverse transcriptase (Clontech) in the presence of oligo (dT) primer (Clontech). PCR was performed using Taq DNA polymerase (EX Taq; Takara Bio) to detect osteocalcin (OCN), bone sialoprotein (BSP), osteopontin (OPN), alkaline phosphatase (ALP), and collagen I (Col1) mRNA using primer designs (synthesized by Sigma-Aldrich) and the PCR condition listed in Table 1. Glyceraldehyde 3-phosphate dehydrogenase (GAPDH) was employed as a housekeeping gene. Preliminary PCRs were performed to determine the annealing temperature and optimal cycle number to yield a linear range of PCR amplification for each primer set. PCR products were visualized on 1.5% agarose gels by ethidium bromide staining. Band intensities were detected and quantified under ultraviolet (UV) light and normalized with reference to GAPDH mRNA.

ALP Activity

ALP activity of the culture was examined at day 7 using image-based and colorimetry-based assays. For the image analysis, cultured cells were incubated with 120 mM Tris buffer (pH 8.4) containing 0.9 mM naphthol AS-MX phosphate and 1.8 mM fast red TR for 30 minutes at 37°C (Sigma Aldrich). For colorimetry, cells were incubated at 37°C for 15 minutes in p-nitrophenylphosphate solution (LabAssay ALP, Wako Pure Chemicals). The amount of nitrophenol released by the enzymatic reaction was measured using an ELISA reader at 405 nm. Each value was standardized by the number of cells in each duplicate culture, counted with a hematocytometer. The value was expressed as ALP activity per unit cell.

Collagen Deposition

Cells were fixed with Bouin's fluid for 1 hour at room temperature. The cultures were treated with 0.2% aqueous phosphomolybdic acid for 1 minute and stained with Sirius red dye (C.I. No. 35780, Pfaltz and Bauer) dissolved in saturated aqueous picric acid (pH 2.0) at a concentration of 100 mg/100 mL for 90 minutes with mild shaking. The cultures were washed with 0.01 N hydrochloric acid for 2 minutes to remove all nonbound dye. Afterward, 600 μL of 0.1 N sodium hydroxide was added to dissolve the staining using a microplate shaker for 30 minutes at room temperature. The optical density (OD) of the solution was then measured using a spectrophotometer at 550 nm against 0.1 N sodium hydroxide as a blank.

OCN Production Analysis

OCN levels in the culture were analyzed immunochemically at day 20 using the OCN detection antibodies (Rat Osteocalcin Assay Kit, Biomedical Technologies) directing against the N-terminal region of OCN. According to the instructions of the manufacturer, the cultures at day 20 were incubated in serum-free α-MEM in a humidified atmosphere of 95% air and 5% CO_2 at 37°C for 48 hours before the assay. After incubation, the supernatant was reacted with a horseradish peroxidase conjugate of a donkey anti-goat IgG and TMB as chromogen. The strength of coloring developed by the reagents was measured by absorbance at 450 nm. The actual concentrations in the culture were calculated based on a parallel OCN standard curve.

Mineralization Assay

Calcium in the culture was dissolved by incubating overnight in 1 mL of 0.5 M HCl solution with gentle shaking. The solution was reacted with o-cresolphthalein complexone in an alkaline medium (Calcium Assay Kit, Cayman Chemical Company). The color intensity of a purple cresolphthalein complexone complex was measured in terms of absorbance at 570 nm using an ELISA reader. To eliminate the influence of TiHA coating on the assay, the OD value on each culture was subtracted by the value on the corresponding disk without cells.

Except for PCR analysis, culture experiments were performed three times for each assay (n = 3).

Statistical Analysis

Surface topographic parameters and wettability were analyzed by Student *t* test between disks with and without TiHA coating within the same titanium substrate. All repeated data in culture experiments were analyzed by Bonferroni multiple comparisons after one-way analysis of variance to determine the differences between each culture condition, using the statistical software (SPSS standard version 16; International Business Machines Corporation). Statistical significance was set at $P < .05$.

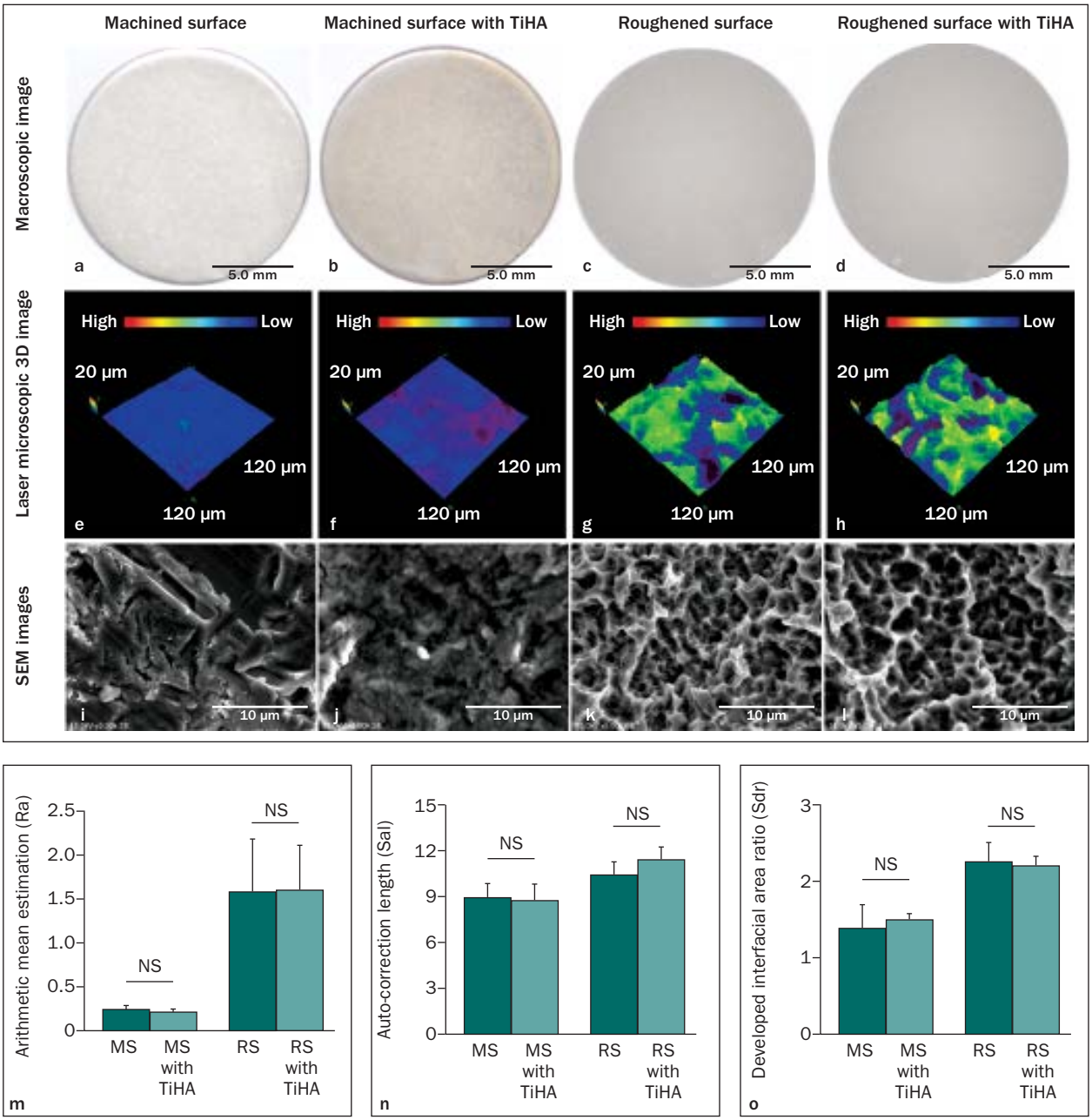

Fig 2 *(a to l)* Representative macroscopic, laser-microscopic 3D, and SEM images of titanium disks with machined or microroughened (SLA) surface with and without TiHA coating. *(m to o)* Quantitative measurements of three parameters of surface topography on titanium disks with machined or microroughened surface with and without TiHA coating. The presented data represent mean ± SD (n = 3). NS = $P > .05$, indicating no statistically significant differences between the titanium disks with and without TiHA coating within the same titanium substrate (Student *t* test); TEM = transmission electron microscopy; TiHA = titanium-doped hydroxyapatite.

RESULTS

Topographic Features of TiHA Coating on Machined and Microroughened Titanium Surfaces

The macroscopic appearance and laser-microscopic three-dimensional (3D) images exhibited that both the machined and microroughened surfaces became slightly and uniformly browned in color (Figs 2a to 2d) but were not changed in micron-level topography after TiHA coating (Figs 2e to 2h). Under SEM observation, the titanium sample with machined surfaces exhibited a smooth-textured but not finely polished appearance, whereas the microroughened titanium surface displayed typical micron-to-submicron scale irregularity with sharp ridges arranged at a micron-scale interval with submicron spikes and pits occupying valleys (Figs 2i to 2l). Uniform coverage of submicron-sized grainy objects was observed on the

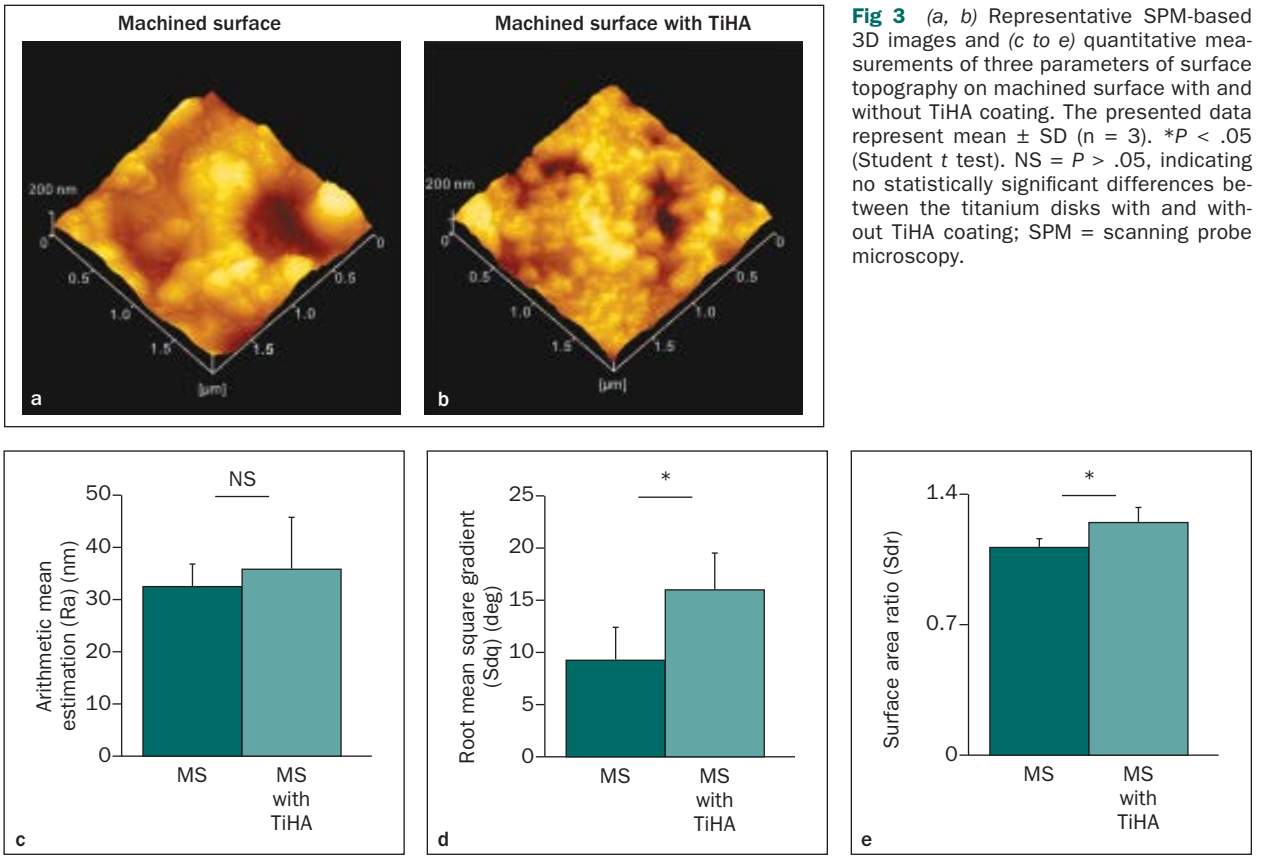

Fig 3 *(a, b)* Representative SPM-based 3D images and *(c to e)* quantitative measurements of three parameters of surface topography on machined surface with and without TiHA coating. The presented data represent mean ± SD (n = 3). *$P < .05$ (Student *t* test). NS = $P > .05$, indicating no statistically significant differences between the titanium disks with and without TiHA coating; SPM = scanning probe microscopy.

machined surface with TiHA coating, whereas the surface topographic change at a submicron level was not recognized on the microroughened surface, even after TiHA coating. There was no significant difference in arithmetic mean estimation (Ra), auto-correlation length (Sal), or developed interfacial area ratio (Sdr) on either the machined or microroughened surface before and after TiHA coating (Figs 2m to 2o). The microroughened surface was consistently higher in such roughness, spatial, and hybrid parameters than the machined surface. Ra, Sal, and Sdr values were approximately 0.2 µm, 8.8 µm, and 1.4 on the machined surfaces and 1.6 µm, 11.0 µm, and 2.2 on the microroughened surfaces, respectively.

SPM analysis on the machined surface revealed that TiHA coating seemed to increase nanoscaled topography (Figs 3a and 3b). The Ra value was not significantly different between the machined surface with or without TiHA coating (Figs 3c to 3e). By contrast, Sdq and Sdr values were increased after TiHA coating.

Changes in Surface Wettability and Chemical Composition on the Machined and Microroughened Titanium Surface After TiHA Coating

The static water contact angle was reduced on both the machined and microroughened titanium surfaces after TiHA coating (Figs 4a and 4b). The machined and microroughened surfaces without TiHA coating exhibited hydrophobicity, where an approximate 90-degree static water contact angle was observed. However, TiHA coating reduced the values on the machined and microroughened surfaces to approximately 50 and 40 degrees, respectively. Under EPMA analysis, a uniform distribution of calcium and phosphorus with entirely reduced titanium detection was observed on both the machined and microroughened titanium surfaces with TiHA coating (Fig 4c). In contrast, high titanium detection with little calcium and phosphorus was observed on both types of surfaces without TiHA coating.

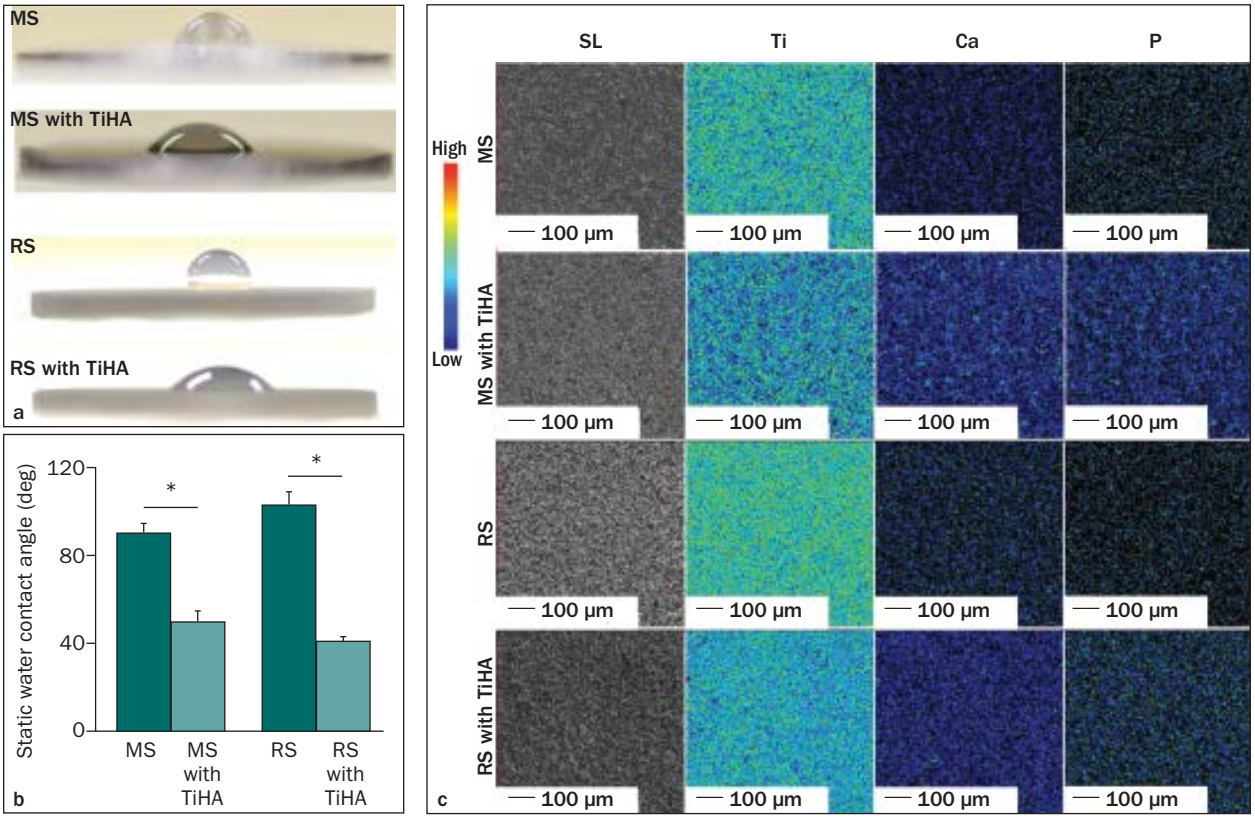

Fig 4 *(a)* Representative macroscopic image showing wettability appearance and *(b)* static water contact angle on titanium disks with machined (MS) or microroughened (SLA) surface (RS) with and without TiHA coating after application of a 10-µL water droplet. Data represent mean ± SD (n = 3). A value of $*P < .05$ represents a significant difference between the titanium disks with and without TiHA coating within the same titanium substrate (Student *t* test). *(c)* Representative EPMA-elemental mapping images of titanium (Ti), calcium (Ca), and phosphorus (P) ions on titanium disks with machined or microroughened surface with and without TiHA coating. Each elemental mapping image corresponds to the spot on the far-left of the SEM images. SEM = scanning electron microscopy; TiHA = titanium-doped hydroxyapatite.

Effects of TiHA Coating on Machined and Microroughened Titanium Surfaces

The number of cells at day 4 was the highest on the TiHA-coated surface by single spin coating with a low concentration of solution (Fig 5a). The TiHA-coated surface with a high concentration of solution or by double spin coating was only 17% or 4% of the value on titanium surface without TiHA coating.

The results of evaluation of the relative cell number by a WST-1 assay at day 2 of the culture were not significantly different between the machined surface with and without TiHA coatings, whereas the value on the microroughened surface with the TiHA coating was higher (Fig 5b). On day 6 of the culture, the cell number on both the machined and microroughened surfaces with the TiHA coating was increased compared with that on the corresponding surfaces without the coating. The relative cell number at day 6 was higher on the machined surface than on the microroughened surface regardless of TiHA coating. TiHA coating increased proliferative activities on day 4 of the culture on both the machined and microroughened surfaces (Fig 5c). In particular, TiHA increased the proliferative activity on the microroughened surface from the lowest level to the level equivalent to that on the machined surface with the coating.

Bone Matrix–Related Gene Expressions on Machined and Microroughened Titanium Surfaces with TiHA Coating

Aside from the TiHA coating, the microroughened surface upregulated all representative bone matrix–related gene markers such as Col1, ALP, OPN, BSP, and OCN to be higher than on the machined surface, almost consistently throughout the culture period of 20 days (Fig 6). On the machined surface, for the culture at day 10, gene markers during the early stage of osteoblastic differentiation, such as Col1, ALP, and BSP, were not different between the surfaces with and without TiHA coating, whereas mid-to-late–stage markers, OPN and OCN,

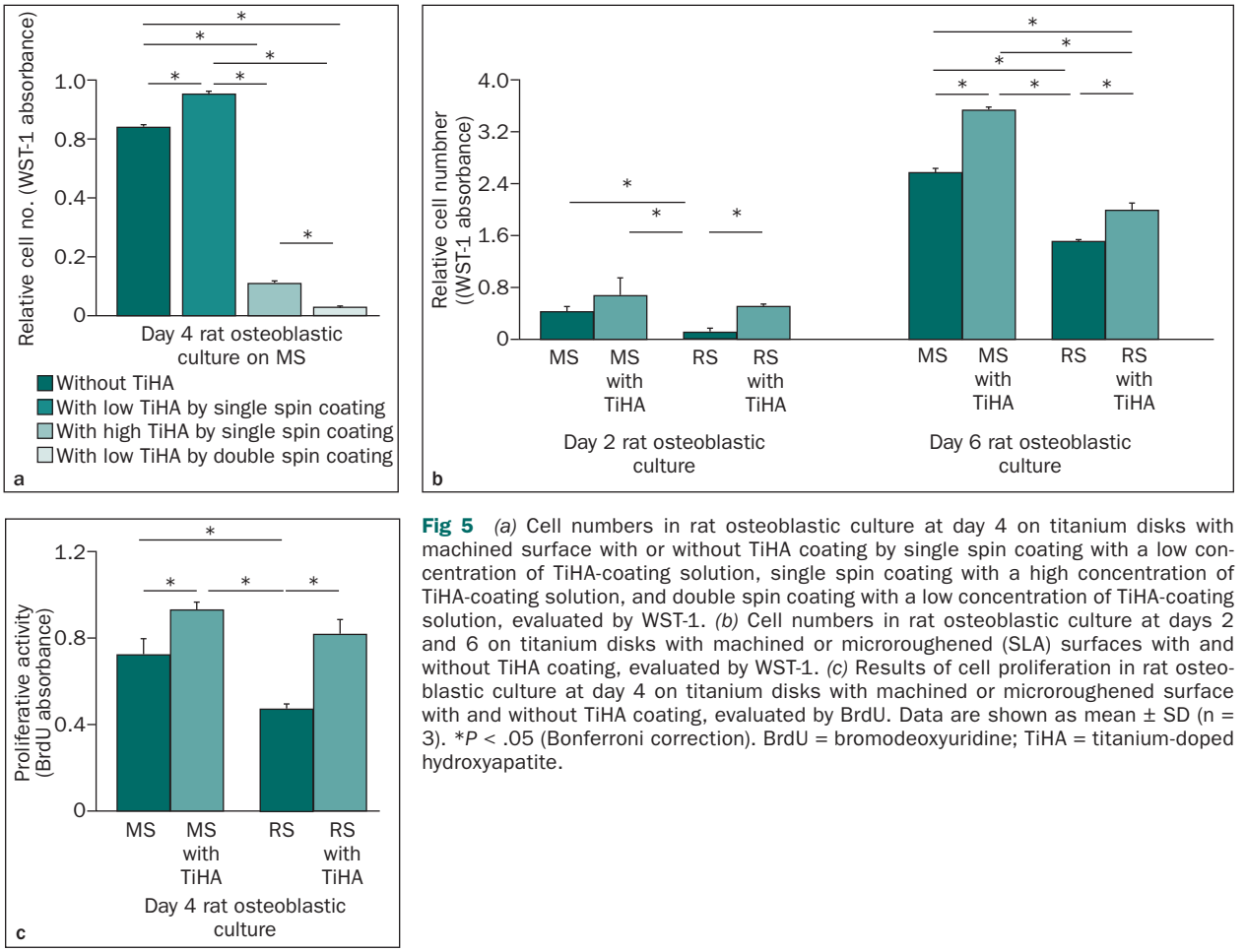

Fig 5 *(a)* Cell numbers in rat osteoblastic culture at day 4 on titanium disks with machined surface with or without TiHA coating by single spin coating with a low concentration of TiHA-coating solution, single spin coating with a high concentration of TiHA-coating solution, and double spin coating with a low concentration of TiHA-coating solution, evaluated by WST-1. *(b)* Cell numbers in rat osteoblastic culture at days 2 and 6 on titanium disks with machined or microroughened (SLA) surfaces with and without TiHA coating, evaluated by WST-1. *(c)* Results of cell proliferation in rat osteoblastic culture at day 4 on titanium disks with machined or microroughened surface with and without TiHA coating, evaluated by BrdU. Data are shown as mean ± SD (n = 3). *$P < .05$ (Bonferroni correction). BrdU = bromodeoxyuridine; TiHA = titanium-doped hydroxyapatite.

were enhanced by TiHA coating. Levels of OPN and OCN expressions on the machined surface with TiHA coating were comparable with those on the microroughened surface at day 10. However, all of the gene markers were hardly expressed on the machined surface with TiHA coating at day 20 compared with steady expressions on the surface without TiHA coating. All of those gene expressions were not different between the microroughened surfaces with and without TiHA coating throughout the culture period of 20 days.

Synthesis and Mineralization of the Bone Matrix on Machined and Microroughened Titanium Surfaces with TiHA Coating

On day 7 of the culture on both the machined and microroughened surfaces, the intensity of ALP staining seemed to be denser on the TiHA-coated surface than on the noncoated surface (Fig 7a). However, the TiHA coating did not increase ALP activity per unit cell in the day 7 culture on either the machined or microroughened surface. Regardless of TiHA coating, the value was higher on the microroughened surface than on the machined surface (Fig 7c). TiHA coating increased collagen deposition by 30% at day 7 on both the machined and microroughened surfaces compared with that on the corresponding surface without the coating (Figs 7b and 7d). The extent of the increase was comparable between machined and roughened surfaces regardless of TiHA coating.

The amount of OCN in the culture at day 20 was higher on the microroughened surface than on the machined surface regardless of TiHA coating (Fig 7e). The machined surface with TiHA coating allowed osteoblastic cells to produce OCN to a level equivalent to that on the microroughened surface without the coating. TiHA coating increased the amount of OCN on the microroughened surface by threefold. Likewise, the amount of calcium in the culture at day 20 was higher on the microroughened surface than on

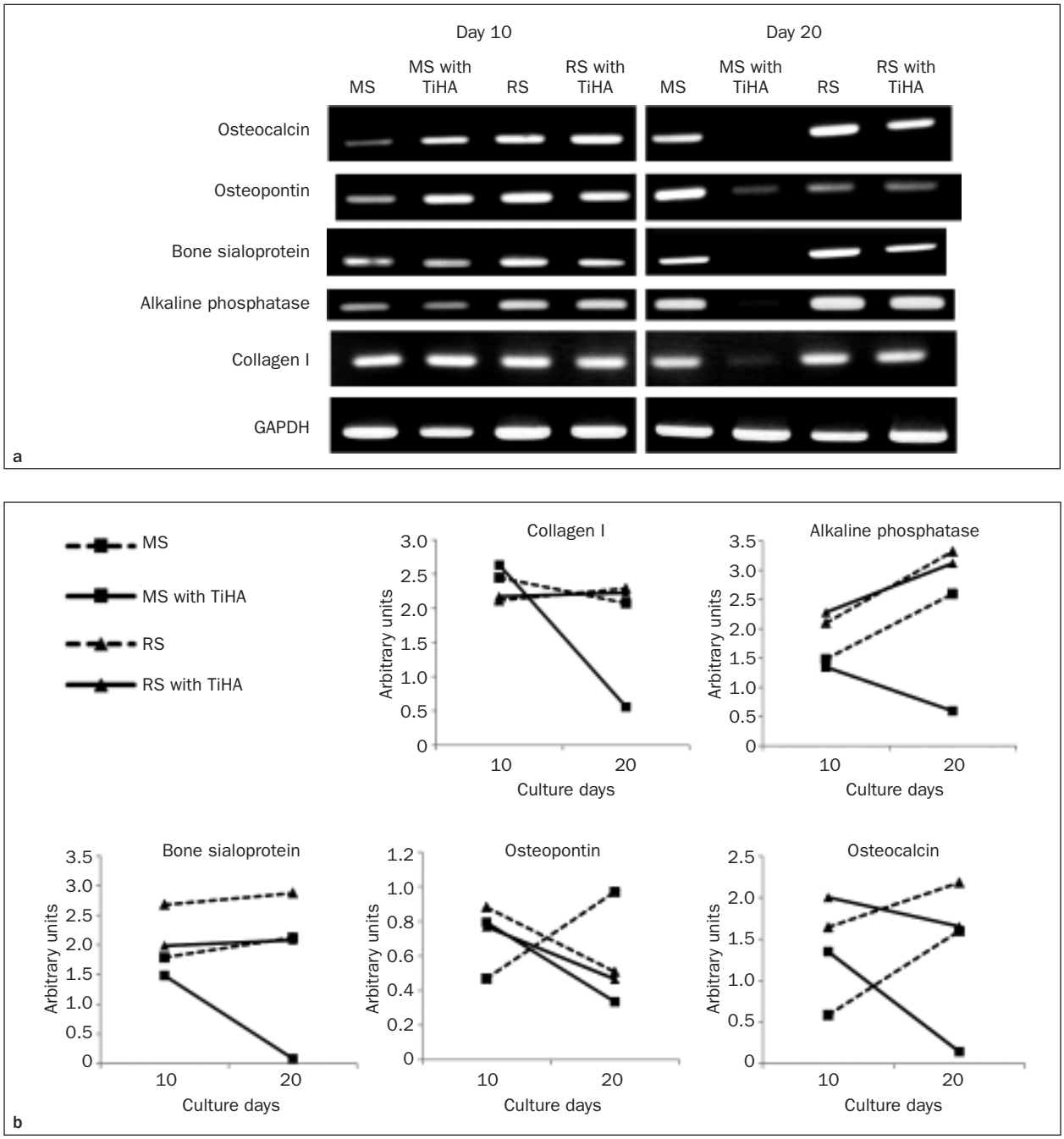

Fig 6 Expression of osteocalcin, osteopontin, bone sialoprotein, alkaline phosphatase, collagen I, and GAPDH genes analyzed by the semiquantitative reverse-transcriptase polymerase chain reaction in rat osteoblastic culture at days 10 and 20 on titanium disks with machined or microroughened (SLA) surfaces with and without TiHA coating. *(a)* Images and *(b)* line graphs indicate intensity of each gene expression and the arbitrary unit against the corresponding GAPDH intensity, respectively. GAPDH = glyceraldehyde 3-phosphate dehydrogenase; TiHA = titanium-doped hydroxyapatite.

the machined surface regardless of TiHA coating (Fig 7f). TiHA coating increased the amount of calcium in the culture on the machined surface to the same degree as that on the microroughened surface without TiHA. The microroughened surface experienced a 30% increase in the amount of calcium in the culture by TiHA coating.

DISCUSSION

The present study is the first to demonstrate the effect of TiHA coating on a titanium surface on osteoblastic cellular function. In the present study, two types of surface topographies, namely, machined and SLA surfaces, were employed as representative of smooth and

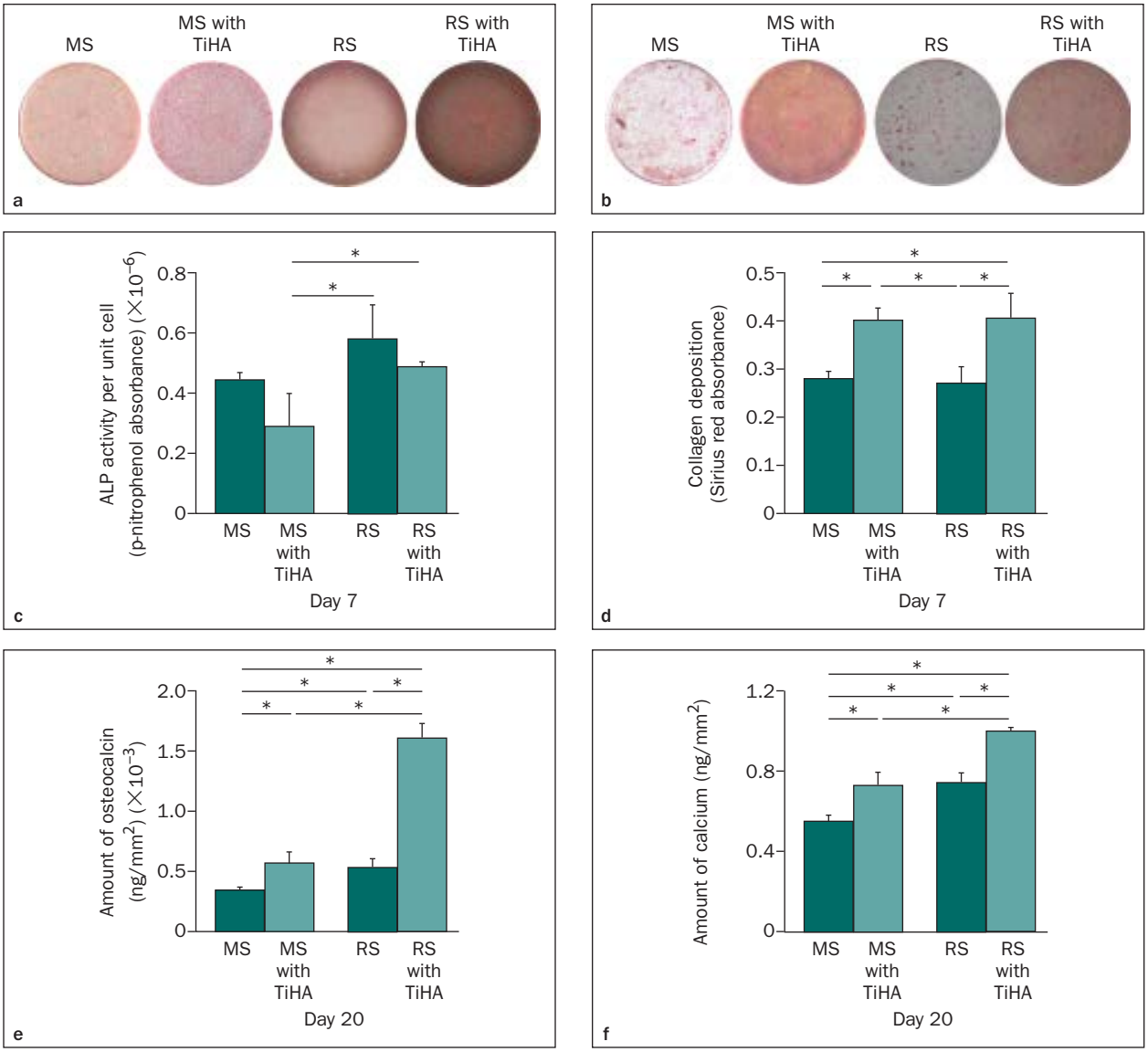

Fig 7 Results of ALP activity *(a)* evaluated by ALP staining and colorimetric determination as ALP activity per unit cell *(c)* and collagen deposition *(b)* by Sirius red staining and the colorimetric value *(d)* in rat osteoblastic culture at day 7 on titanium disks with machined (MS) or microroughened (SLA) surface (RS) with and without TiHA coating. Results of quantifications of *(e)* osteocalcin and *(f)* calcium deposition in rat osteoblastic culture at day 20 on titanium disks with machined or microroughened surfaces with and without TiHA coating. Data are shown as the mean ± SD (n = 3). *$P < .05$ (Bonferroni correction). ALP = alkaline phosphatase; TiHA = titanium-doped hydroxyapatite.

microroughened titanium surfaces, respectively. It is well-known that a titanium surface with micron-to-submicron roughness restricts proliferation but activates osteoblastic attachment and differentiation.[25,26] Proliferative activity and the progress of osteoblastic differentiation generally exhibited an inverse relationship.[27,28] Many studies have reported that a micron-to-submicron roughened titanium surface enhances production and mineralization of the bone matrix to a greater extent than a smooth titanium surface such as a turned or machined surface,[29–35] and hence, upgraded osseointegration capability.[32,33,36] Besides TiHA coating, in the present study, rat osteoblastic cells reduced proliferative activity but increased osteoblastic differentiation on the microroughened surface compared with those on the machined surface, which was observed as enhancements of the bone matrix expression and matrix mineralization at both the genetic and protein levels. In light of content and criterion-related validities, the titanium surface topographies used in the present study could be regarded as clinically relevant, assuredly effective, and universally comparable model substrates, and allow the realistic evaluation of the biologic performance of TiHA coating as adjunct modification on an existing titanium surface.

Table 1 Details of Primers and Condition of Reverse Transcription Polymerase Chain Reaction

	Sequence (5'–3')	Annealing temperature	No. of cycles	Size of product (bp)
Osteocalcin	GTCCCACACAGCAACTCG CCAAAGCTGAAGCTGCCG	61	26	380
Bone sialoprotein	CAGGAGGCGGAGGCAGAG CATACTCAACCGTGCTGC	63	27	487
Osteopontin	GATTATAGTGACACAGAC AGCAGGAATACTAACTGC	51	19	287
Alkaline phosphatase	GACAAGAAGCCCTTCACAGC GGGGGATGTAGTTCTGCTCA	63	30	229
Collagen I	GGCAACAGTCGATTCACC AGGGCCAATGTCCATTCC	58	28	177
GAPDH	TGAAGGTCGGTGTCAACGGATTTGGC CATGTAGGCCATGAGGTCCACCAC	67	27	983

EPMA analysis detected a uniform and dense distribution of calcium and phosphorus ions throughout both the machined and microroughened surfaces with TiHA. Those ions originated from components within TiHA. Therefore, the TiHA coating method was regarded to be a complete and uniform TiHA covering over the entire area of the titanium surface regardless of surface topography. This suggested that osteoblastic cells were always exposed to the physicochemical properties of TiHA. When considering the effect of HA material on osteoblastic function, it must be distinguished whether the HA material was water soluble or insoluble. Water-soluble HA material releases calcium ions that could modulate osteoblastic function,[37] whereas insoluble HA as bipolar material is expected to attract protein by chemical bond[38] and electrostatic attraction between Ca^{2+} and PO_4^{3-} sites in the HA crystal and COO^- and NH_2^+ in amino acids.[39] Previous material studies regarding TiHA demonstrated that the cation (titanium and calcium)/phosphorus ratio of TiHA was 1.62 to 1.65,[40] which indicated that chemical stability of TiHA was similar to stoichiometric HA (Ca/P = 1.67) and that TiHA was hardly water soluble. In fact, ionic concentrations of Ca^{2+}, PO_4^{3-}, and Ti^{4+} dissolved from the TiHA particle in a 1×10^{-4} KCl solution at 15°C for 1 day were approximately 30, 200, and 1.0 μmol/m^2, respectively.[40,41] Therefore, TiHA might function as a bipolar material to adhere to protein. In addition, TiHA coating changed water wettability on both machined and microroughened titanium surfaces from hydrophobic (contact angle ≥ 90 degrees) to hydrophilic status (contact angle ≈ 40 degrees) in the present study. A hydrophilic surface facilitates extracellular matrix proteins in the serum within the culture media to be positioned close to the surface.[14] Determination of interaction of TiHA coating with protein deposition manner and subsequent expression pattern of cell adhesion molecules and proliferative activity of osteoblastic cells would be of great interest for future research.

Proliferative activity and progress of differentiation in osteoblastic lineage will exhibit an inverse relationship as a basic biologic rule.[27,28] TiHA coating did not change the ALP activity and gene expression pattern of bone matrix on the microroughened surface. On the machined surface, TiHA coating upregulated expressions of the mid-to-late–stage markers, OPN and OCN, on day 10 but nearly terminated all gene expressions by day 20 of the present study. However, osteoblastic cells increased the amount of collagen, OCN, and calcium in the culture on both the machined and microroughened surfaces by TiHA coating. During the earlier culture period, TiHA increased the attached cell number and cellular proliferative activity on both the machined and microroughened surfaces. All of these results suggested that regardless of the topography, osteoblastic cells on the titanium surface with TiHA coating were activated in cellular proliferation but not suppressed in differentiation against a basic biologic rule. This should be a theoretical and reasonable solution to the question of why the machined and microroughened surfaces with TiHA coating could enhance extracellular matrix production and mineralization in an osteoblastic culture without upregulation of the bone matrix gene expressions.

The other question was how TiHA coating enhanced osteoblastic proliferation on the titanium surface. Surface topographic analysis could not detect apparent topographic modification at the micron level on the microroughened surface after TiHA coating. In contrast, TiHA coating changed nanotopography on the machined surface detected as submicron-sized grainy objects observed under SEM. However, SPM-based nanosurface analysis demonstrated that TiHA slightly increased Sdr and Sdq, but not Ra values. This meant that TiHA slightly increased the surface area and irregularity of the titanium surface without a change of roughness depth. Previous articles indicated that submicron-sized convexoconcave with sharp, anisotropic, and densely

packed edges and spikes, was favorable for activation of osteoblastic function.[2,42] This indicated that activation of osteoblastic proliferation on the TiHA-coated titanium surfaces was not attributed to a slight change of nanotopography with grainy objects. Therefore, the effect of TiHA coating on osteoblastic function can possibly be attributed to the other surface properties such as physicochemical properties.

It was reported that the titanium implant coated with relatively dense nano-HA spikes was higher in bone-to-implant contact ratio than the noncoated implant in a rabbit femur model.[43,44] However, an increase of roughness with nano-HA coating did not always upgrade osseointegration capability,[45] in contrast with the well-known influence of the machined and microroughened titanium surfaces on osteoblastic proliferation and differentiation during the osseointegration process.[46] Moreover, osteoblastic cellular responses on surface wettability were also infinite in variety within the literature. A previous culture study demonstrated that a superhydrophilic status on a machined or microroughened titanium surface did not always enhance osteoblastic attachment.[14] By contrast, it was demonstrated that a chemically modified microroughened surface with superhydrophilicity reduced the cell number but increased production of the extracellular matrix.[47] There was not as much hydrophilicity on the TiHA-coated titanium surface as on superhydrophilic surfaces such as chemically modified microroughened[48] or photofunctionalized titanium surfaces.[49] However, TiHA coating also had inherent bipolarity as HA material. Those observations implied that enhancement of proliferative activity without deterioration of osteoblastic differentiation was attributed to synergistic effects of such dual physicochemical properties and an inherent surface topography. Association of nanoroughness and physicochemical properties in osseointegration capability remained to be fully elucidated.

There were some limitations associated with the present study in light of clinical application. First, although this in vitro study demonstrated an upgrade of osseointegration potential of a clinically relevant titanium surface with a microroughened surface by TiHA coating, the actual osseointegration capability of TiHA should be determined by a preclinical animal model. In addition, the toughness of TiHA coating for the inflammatory situation or delamination forces in local tissue should be determined by physicochemical erosion and mechanical peering tests, because traditionally, the HA surface has suffered from those unfavorable situations.[50] However, the thickness of TiHA coating in the present study was 150 to 200 nm; the degree of thinness indicated that TiHA coating could avoid loading concentration for delamination within the coating layer and at the interface between the coating and titanium substrate, which is seen on the traditional HA coating with a several dozen–micron thickness.[51,52] Moreover, TiHA inherently exerts active antimicrobial capability and did not require UV irradiation, in contrast to the TiO_2-mediated photocatalyst.[22] TiHA coating might reduce susceptibility of the titanium implant to peri-implant infection, in contrast with the nano-HA coating failing to overcome the inherent bacterial affinity of the titanium surface.[53] Application of this TiHA coating for modification of the zirconia surface is also of great interest in light of overcoming outstanding issues in the field of implant dentistry. Despite requirements of further material and biologic evidence regarding clinical effectiveness and safety, TiHA coating could pave the way to a new era in titanium surface modification.

CONCLUSIONS

Regardless of the topography of titanium substrate, TiHA coating enhanced cellular proliferation, without deterioration of cellular differentiation, and subsequent extracellular matrix formation and matrix mineralization in rat bone marrow–derived osteoblastic culture on the surface, possibly through adjunction of calcium and phosphate ions and acquirement of hydrophilicity on the titanium surface.

ACKNOWLEDGMENTS

The authors appreciate Eiko Watanabe (HRC research associate) for her assistance with EPMA analysis. This work was supported by Grant-in-Aid for Scientific Research (C) of Japan, 2014-2016 (grant number 26462978). Masato Wakamura is an employee in Fujitsu Laboratories Ltd. The other authors have no conflict of interest.

REFERENCES

1. Tomisa AP, Launey ME, Lee JS, Mankani MH, Wegst UG, Saiz E. Nanotechnology approaches to improve dental implants. Int J Oral Maxillofac Implants 2011;26(suppl):s25–s44.
2. Gittens RA, Olivares-Navarrete R, Schwartz Z, Boyan BD. Implant osseointegration and the role of microroughness and nanostructures: Lessons for spine implants. Acta Biomater 2014;10:3363–3371.
3. Gittens RA, Scheideler L, Rupp F, et al. A review on the wettability of dental implant surfaces II: Biological and clinical aspects. Acta Biomater 2014;10:2907–2918.
4. Yamada M, Ueno T, Minamikawa H, Ikeda T, Nakagawa K, Ogawa T. Early-stage osseointegration capability of a submicrofeatured titanium surface created by microroughening and anodic oxidation. Clin Oral Implants Res 2013;24:991–1001.
5. Schwartz Z, Raz P, Zhao G, et al. Effect of micrometer-scale roughness of the surface of Ti6Al4V pedicle screws in vitro and in vivo. J Bone Joint Surg Am 2008;90:2485–2498.
6. Xu LC, Siedlecki CA. Effects of surface wettability and contact time on protein adhesion to biomaterial surfaces. Biomaterials 2007;28:3273–3283.

7. Wilson CJ, Clegg RE, Leavesley DI, Pearcy MJ. Mediation of biomaterial-cell interactions by adsorbed proteins: A review. Tissue Eng 2005;11:1–18.
8. Brash JL, Horbett TA. Proteins at interfaces: An overview. In: Horbett TA, Brash JL. (ed). Proteins at Interfaces II: Fundamentals and Applications. Washington, DC: American Chemical Society, 1995:1–23.
9. Keselowsky BG, Wang L, Schwartz Z, Garcia AJ, Boyan BD. Integrin alpha(5) controls osteoblastic proliferation and differentiation responses to titanium substrates presenting different roughness characteristics in a roughness independent manner. J Biomed Mater Res A 2007;80:700–710.
10. Arima Y, Iwata H. Effect of wettability and surface functional groups on protein adsorption and cell adhesion using well-defined mixed self-assembled monolayers. Biomaterials 2007;28:3074–3082.
11. Scotchford CA, Gilmore CP, Cooper E, Leggett GJ, Downes S. Protein adsorption and human osteoblast-like cell attachment and growth on alkylthiol on gold self-assembled monolayers. J Biomed Mater Res 2002;59:84–99.
12. Webb K, Hlady V, Tresco PA. Relationships among cell attachment, spreading, cytoskeletal organization, and migration rate for anchorage-dependent cells on model surfaces. J Biomed Mater Res 2000;49:362–368.
13. Amphlett GW, Hrinda ME. The binding of calcium to human fibronectin. Biochem Biophys Res Commun 1983;111:1045–1053.
14. Uchiyama H, Yamada M, Ishizaki K, Sakurai K. Specific ultraviolet-C irradiation energy for functionalization of titanium surface to increase osteoblastic cellular attachment. J Biomater Appl 2014;28:1419–1429.
15. Buser D, Broggini N, Wieland M, et al. Enhanced bone apposition to a chemically modified SLA titanium surface. J Dent Res 2004;83:529–533.
16. Yasukawa A, Higashijima M, Kandori K, Ishikawa T. Preparation and characterization of cadmium–calcium hydroxyapatite solid solution particles. Colloid Surface A 2005;268:111–117.
17. Laurencin D, Almora-Barrios N, de Leeuw NH, et al. Magnesium incorporation into hydroxyapatite. Biomaterials 2011;32:1826–1837.
18. Yasukawa A, Ueda E, Kandori K, Ishikawa T. Preparation and characterization of carbonated barium-calcium hydroxyapatite solid solutions. J Colloid Interface Sci 2005;288:468–474.
19. Yasukawa A, Kamiuchi K, Yokoyama T, Ishikawa T. Preparation of lead-calcium hydroxyapatite solid solutions by a wet method using acetamide. J Solid State Chem 2002;163:27–32.
20. Wakamura M, Kandori K, Ishikawa T. Surface structure and composition of calcium hydroxyapatites substituted with Al(III), La(III) and Fe(III) ions. Colloid Surface A 2000;164:297–305.
21. Iconaru SL, Chapon P, Le Coustumer P, Predoi D. Antimicrobial activity of thin solid films of silver doped hydroxyapatite prepared by sol-gel method. ScientificWorldJournal 2014;2014:165351.
22. Wakamura M, Hashimoto K, Watanabe T. Photocatalysis by calcium hydroxyapatite modified with Ti(IV): Albumin decomposition and bactericidal effect. Langmuir 2003;19:3428–3431.
23. Watanabe T, Yoshida N. Wettability control of a solid surface by utilizing photocatalysis. Chem Rec 2008;8:279–290.
24. Kandori K, Oketani M, Wakamura M. Decomposition of proteins by photocatalytic Ti(IV)-doped calcium hydroxyapatite particles. Colloids Surf B Biointerfaces 2013;102:908–914.
25. Bacáková L, Starý V, Kofronová O, Lisá V. Polishing and coating carbon fiber-reinforced carbon composites with a carbon-titanium layer enhances adhesion and growth of osteoblast-like MG63 cells and vascular smooth muscle cells in vitro. J Biomed Mater Res 2001;54:567–578.
26. Balani K, Anderson R, Laha T, et al. Plasma-sprayed carbon nanotube reinforced hydroxyapatite coatings and their interaction with human osteoblasts in vitro. Biomaterials 2007;28:618–624.
27. Malaval L, Liu F, Roche P, Aubin JE. Kinetics of osteoprogenitor proliferation and osteoblast differentiation in vitro. J Cell Biochem 1999;74:616–627.
28. Stein GS, Lian JB, Owen TA. Relationship of cell growth to the regulation of tissue-specific gene expression during osteoblast differentiation. FASEB J 1990;4:3111–3123.
29. Zhao G, Zinger O, Schwartz Z, Wieland M, Landolt D, Boyan BD. Osteoblast-like cells are sensitive to submicron-scale surface structure. Clin Oral Implants Res 2006;17:258–264.
30. Zinger O, Zhao G, Schwartz Z, et al. Differential regulation of osteoblasts by substrate microstructural features. Biomaterials 2005;26:1837–1847.
31. Nakamura H, Saruwatari L, Aita H, Takeuchi K, Ogawa T. Molecular and biomechanical characterization of mineralized tissue by dental pulp cells on titanium. J Dent Res 2005;84:515–520.
32. Takeuchi K, Saruwatari L, Nakamura HK, Yang JM, Ogawa T. Enhanced intrinsic biomechanical properties of osteoblastic mineralized tissue on roughened titanium surface. J Biomed Mater Res A 2005;72:296–305.
33. Butz F, Aita H, Wang CJ, Ogawa T. Harder and stiffer bone osseointegrated to roughened titanium. J Dent Res 2006;85:560–565.
34. Mendonça G, Mendonça DB, Simões LG, et al. The effects of implant surface nanoscale features on osteoblast-specific gene expression. Biomaterials 2009;30:4053–4062.
35. de Oliveira PT, Nanci A. Nanotexturing of titanium-based surfaces upregulates expression of bone sialoprotein and osteopontin by cultured osteogenic cells. Biomaterials 2004;25:403–413.
36. Ogawa T, Ozawa S, Shih JH, et al. Biomechanical evaluation of osseous implants having different surface topographies in rats. J Dent Res 2000;79:1857–1863.
37. Beck GR Jr. Inorganic phosphate as a signaling molecule in osteoblast differentiation. J Cell Biochem 2003;90:234–243.
38. Gorbunoff MJ. The interaction of proteins with hydroxyapatite. I. Role of protein charge and structure. Anal Biochem 1984;136:425–432.
39. Gorbunoff MJ. The interaction of proteins with hydroxyapatite. II. Role of acidic and basic groups. Anal Biochem 1984;136:433–439.
40. Kandori K, Kuroda T, Wakamura M. Protein adsorption behaviors onto photocatalytic Ti(IV)-doped calcium hydroxyapatite particles. Colloids Surf B Biointerfaces 2011;87:472–479.
41. Kandori K, Oketani M, Wakamura M. Effects of Ti(IV) substitution on protein adsorption behaviors of calcium hydroxyapatite particles. Colloids Surf B Biointerfaces 2013;101:68–73.
42. Mendonça G, Mendonça DB, Aragão FJ, Cooper LF. Advancing dental implant surface technology—From micron- to nanotopography. Biomaterials 2008;29:3822–3835.
43. Meirelles L, Arvidsson A, Andersson M, Kjellin P, Albrektsson T, Wennerberg A. Nano hydroxyapatite structures influence early bone formation. J Biomed Mater Res A 2008;87:299–307.
44. Jimbo R, Coelho PG, Vandeweghe S, et al. Histological and three-dimensional evaluation of osseointegration to nanostructured calcium phosphate-coated implants. Acta Biomater 2011;7:4229–4234.
45. Jimbo R, Sotres J, Johansson C, Breding K, Currie F, Wennerberg A. The biological response to three different nanostructures applied on smooth implant surfaces. Clin Oral Implants Res 2012;23:706–712.
46. Ogawa T, Nishimura I. Different bone integration profiles of turned and acid-etched implants associated with modulated expression of extracellular matrix genes. Int J Oral Maxillofac Implants 2003;18:200–210.
47. Zhao G, Schwartz Z, Wieland M, et al. High surface energy enhances cell response to titanium substrate microstructure. J Biomed Mater Res A 2005;74:49–58.
48. Rupp F, Scheideler L, Eichler M, Geis-Gerstorfer J. Wetting behavior of dental implants. Int J Oral Maxillofac Implants 2011;26:1256–1266.
49. Funato A, Yamada M, Ogawa T. Success rate, healing time, and implant stability of photofunctionalized dental implants. Int J Oral Maxillofac Implants 2013;28:1261–1271.
50. Piattelli A, Cosci F, Scarano A, Trisi P. Localized chronic suppurative bone infection as a sequel of peri-implantitis in a hydroxyapatite-coated dental implant. Biomaterials 1995;16:917–920.
51. Geesink RG. Osteoconductive coatings for total joint arthroplasty. Clin Orthop Relat Res 2002;395:53–65.
52. Gross KA, Berndt CC, Herman H. Amorphous phase formation in plasma-sprayed hydroxyapatite coatings. J Biomed Mater Res 1998;39:407–414.
53. Westas E, Gillstedt M, Lönn-Stensrud J, Bruzell E, Andersson M. Biofilm formation on nanostructured hydroxyapatite-coated titanium. J Biomed Mater Res A 2014;102:1063–1070.